Macromolecular Materials and Engineering
Open Access
www.mame-journal.de

A Facile and Green Microwave-Assisted Strategy to Induce Surface Properties on Complex-Shape Polymeric 3D Printed Structures

Gustavo Gonzalez, María Arévalo, Annalisa Chiappone, Enrique Martínez Campos, Candido Fabrizio Pirri, Ignazio Roppolo, and Paula Bosch*

Light- induced polymeric 3D printing is becoming a well-established fabrication method, showing manifold advantages such as control of the local chemistry of the manufactured devices. It can be considered a green technology, since the parts are produced when needed and with minimum amount of materials. In this work 3D printing is combined with another green technology, microwave-assisted reaction, to fabricate objects of complex geometry with controllable surface properties, exploiting the presence of remaining functional groups on the surface of 3D printed specimens. In this context, surface functionalization with different amines is studied, optimizing formulations, reaction times, and avoiding surface deterioration. Then, two different applications are investigated. MW-functionalized filter-type structures have been tested against *Staphylococcus aureus* bacteria, showing high bactericidal activity on the surface along all areas of the complex-shaped structure. Second, a fluidic chip composed of three separated channels is 3D printed, filled with different amine-reactive dyes (dansyl and eosine derivatives), and made to react simultaneously. Complete and independent functionalization of the surface of the three channels is achieved only after 2 min of irradiation. This study demonstrates that light induced 3D printing and microwave-induced chemistry can be used together effectively, and used to produce functional devices.

1. Introduction

In recent years, 3D printing is going far beyond its initial purposes, moving from rapid prototyping and modeling to a suitable technique to fabricate functional printed objects. These can be produced on demand with limited materials and energy consumption, which makes 3D printing part of the green technologies.[1] 3D printing versatility is based on twofold levels: technology and materials. The former enables the design and the production of structures with superior complex shapes, that can be used, for instance, in mechanics, aerospace, or medicine modeling.[2,3] Whilst from the material point of view, one can produce functional parts with enhanced performances and additional properties and features (e.g., electrical conductivity magnetic or optical properties).[4–6] The 3D printing revolutionizing premise relies on the combination of these two aspects. Such shape/materials synergistic effect is nowadays employed to fabricate innovative devices for different applications, including medicine, robotics, electronics, optics, and catalysis among others.[7,8]

G. Gonzalez, C. F. Pirri, I. Roppolo
Department of Applied Science and Technology
Polytechnic University of Turin
C.so Duca Degli Abruzzi 24, Turin 10129, Italy
E-mail: ignazio.roppolo@polito.it

M. Arévalo, E. Martínez Campos, P. Bosch
Departamento de Química Macromolecular Aplicada
Institute of Polymer Science and Technology, Spanish National Research Council (CSIC)
C/Juan de la Cierva 3, Madrid 28006, Spain

A. Chiappone
Department of Chemical and Geological Sciences
University of Cagliari, Monserrato University Complex
S.S. 554 bivio Sestu, Monserrato 09042, Italy

M. Arévalo, E. Martínez Campos
Group of Organic Synthesis and Bioevaluation
Multidisciplinary Institute, Complutense University of Madrid,
Associated Unit to the ICTP-IQM-CSIC
Paseo Juan XXIII n 1, Madrid 28040, Spain

C. F. Pirri, I. Roppolo
Center for Sustainable Future Technology @Polito
Italian Institute of Technology
Via Livorno 60, Turin 10144, Italy

C. F. Pirri, I. Roppolo
PolitoBIOMed Lab
Polytechnic University of Turin
C.so Castelfidardo 30/A, Turin 10129, Italy

DOI: 10.1002/mame.202300118

Particularly, 3D printed parts with enhanced surface properties are extremely appealing in the biology, biotechnology, and chemistry fields. In this context, light activated 3D printing is particularly suitable since, operating with liquid resins, allows an easy control of the materials properties.[9,10] Different works reported the addition of functional additives or nanoparticles into a photopolymerizable resin to fabricate structures with surface-exposed molecules that can be used, for instance, as anchoring points during a second step of functionalization.[11] This surface functionalization approach can be of great advantage since post-functionalization can be carried out on demand and with different types of molecules.[12–14] The surface functionalization of polymeric objects can be obtained exploiting several techniques, including plasma,[15] deposition processing,[16] grafting in standard chemical batches,[17] and microwave-assisted reactions.[18,19] Among these, microwave (MW) irradiation procedures are considered outstanding since they allot to shorten the reaction times, maintaining (or increasing) the yield of reaction products. Besides, MW is a low energy-consuming, inexpensive, and facile technique, that minimizes the by-product formation;[20] which can lead to classify it as well as green technology.[1] With MW irradiation procedures one can achieve specific chemical reactions between functional groups by coupling acrylic double bonds or epoxy groups with amine-terminated compounds,[21,22] which can be controlled by adjusting the MW settings like the energy delivered to the system and the time of MW exposure.

In this work, we combined the 3D printing versatility to produce complex-shaped and customized structures with the benefits of microwave irradiation to surface functionalize the printed samples in an easy, fast, and environmentally-friendly way. The functionalization of 3D printed parts is investigated proceeding with the high-yield microwave-induced strategy taking advantage of the remaining functional groups on the surface of 3D printed specimens. Four different acrylate/epoxy formulations, based on polyethylene glycol diacrylate (PEGDA) and glycidyl methacrylate (GMA), are prepared and processed using a digital light processing (DLP)-3D printing technique. PEGDA250 was selected as a difunctional monomer since its low molecular weight assures a high degree of crosslinking, and then, a low swellability in water. This aspect is particularly important to avoid failure of the 3D printed structure during post processing.[23,24] Glycidyl methacrylate (GMA) monomer was used to incorporate epoxy groups into the polymeric structures by copolymerization with PEGDA250 during the 3D printing step.[25] The active functional groups of the printed parts (epoxy and unreacted acrylate) can be used as an anchoring point for surface functionalization, in this case with aliphatic amines, through nucleophilic ring-opening and Michael reactions. Typically, both reactions (between amines and epoxy or acrylate functionalities) are usually thermally activated and can even proceed at room temperature in the appropriate conditions (pH catalyzed or photo-triggered).[26–28] Instead, here, this reaction will be induced using microwave irradiation to shorten the reaction times.[21,29] The extent of surface post-printing functionalization is evaluated by varying experimental parameters, such as the acrylate/epoxy concentration and irradiation conditions. A series of experimental analyses are performed for optimizing the microwave-assisted functionalization procedure to find a compromise between the desired surface properties and the final sample's properties. Considering amines' antimicrobial activity, the antibacterial behavior of the MW-treated 3D printed samples is evaluated against *Staphylococcus aureus*. Considering the versatility to produce complex and customized objects by 3D printing techniques and the great reactivity of amine functional groups as well, a three-parallel-channel 3D-printed device was fabricated to functionalize the channel surface with two different amine-reactive molecules, simultaneously but independently, in a second functionalization step.

2. Results and Discussion

2.1. 3D Printing PEGDA250 and GMA Samples

Starting from previous results,[25] the four PEGDA/GMA formulations (containing 1 wt% of phenyl *bis*(2,4,6-trimethylbenzoyl)phosphine oxide BAPO and 0.01 wt% of disperse Red 1 methacrylateDR1-MA dye each) were successfully processed using the Asiga 3D-DLP printer and following the printing settings shown in **Table 1**. Basic and complex-shaped samples were successfully fabricated, see Figure S1a,b, Supporting Information. As mentioned, GMA monomer was used to incorporate epoxy groups into the polymeric structures through copolymerization with PEGDA250 during the 3D printing step. In this way, the epoxy ring can react with other molecules, such as aliphatic amines, in the second step of functionalization using microwaves, as represented in **Figure 1**a.

After the 3D printed step, ATR-FTIR spectra were recorded on the samples, confirming the presence of epoxy functionalities (see Figure S2, Supporting Information). This proves that epoxy rings did not react, as expected, during the photopolymerization process. The FTIR spectra showed the presence of acrylate double bonds on the printed samples, indicating that C=C groups remain also active after printing. Therefore, both the non-reacted acrylate and unreacted epoxy functionalities are available on the surface and can react with aliphatic polyamines (e.g., diethylenetriamine (DETA), hyperbranched polyethyleneimine with low molecular weight –PEI600 or high molecular weight –PEI10k) to functionalize the surface of the sample. These reactions have been widely reported in the literature, and they proceed through the nucleophilic attack of the electron pair of the N atom to both acrylate and glycidyl groups.[28,30,31] Although, in this case, the reaction will be assisted by microwave irradiation.

2.2. Microwave-Assisted Surface Modification

The surface modification of the 3D printed samples was carried out under microwave radiation, as described in the Experimental Section. The reaction time varied between 30 s and 20 min, depending on the type of amine used. Flat sample discs (0.9 cm diameter and 0.1 cm height) were used to optimize reaction's conditions as they were easier to handle and to analyze than complex structures. After the washing procedure, the samples' surfaces were tested using ATR-FTIR. The ATR-IR spectra showed the disappearance of both 905 cm^{-1} (glycidyl) and 810 cm^{-1} (acrylate) bands when increasing the reaction times. Simultaneously, the appearance of two strong bands confirmed the grafting of the polyethyeneamines onto the sample surface: one

Table 1. Weight percent (%), molar acrylate/epoxy ratio for each PEGDA250 and GMA formulation, and the 3D printing settings used for each formulation with 50 µm of slicing thickness.

Formulation	PEGDA250 [wt%]	GMA [wt%]	Acrylate/epoxy molar ratio	Exposure time [s layer^{-1}]	Initial exposure time [s layer^{-1}][a)]
PEGDA250	100	—	—	1.2	3
9:1 PEGDA250/GMA	90	10	10.23:1	1.5	3
7:3 PEGDA250/GMA	70	30	2.65:1	5	9
5:5 PEGAD250/GMA	50	50	1.14:1	10	14

[a)] Irradiation time for the first three layers to guarantee an adequate adhesion of the parts.

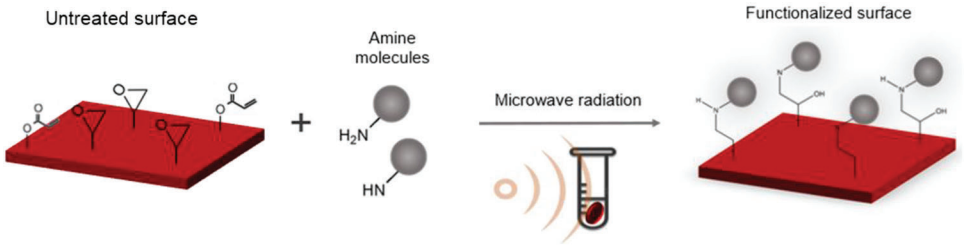

Figure 1. A scheme of the surface functionalization procedure approached in this work using microwave radiation on 3D printed polymeric samples.

large band at 3600–3200 cm^{-1} (superimposition of O–H st and N–H st) and a second in the 3000–2800 cm^{-1} regions (C–H st). On the other hand, the acrylate double-bond band at 810 cm^{-1} decreases considerably during the MW treatment: this can be attributed to the reaction between the C=C double-bonds with primary/secondary amines, but also to the thermal contribution related to the microwave radiation which induce bond opening, as already reported in literature,[32,33] and as detailed in Figure S3, Supporting Information. Differences in kinetics were found for the different amine structures, but the trend is identical for all. As an example, results in 5:5 PEGDA250/GMA (formulation with the higher content of GMA) are shown in **Figure 2**. The reaction times play a key role in the MW functionalization step and, as shown in Figure 2 (right column), a short time of MW irradiation can be sufficient to completely functionalize the surface of the samples with amines. In details, both the surface reactive groups (acrylic double bond band at 810 cm^{-1} and epoxy band at 905 cm^{-1}) and the newly formed bonds (C–H st band at 2935, O–H st at 3500 cm^{-1} and N–H st band at 3290 cm^{-1}) reach a plateau after a variable time of MW irradiation. The epoxy/acrylate conversion can be increased, increasing the MW reaction times, but in some samples evident surface deterioration after prolonged times of MW treatment was noticed (Figure S1c, Supporting Information). Hence, it is important to establish the minimum MW irradiation time necessary to functionalize the samples' surface with amines. Using PEI600, 30 s of MW reaction was sufficient to functionalize the PEGDA/GMA samples as shown in Figure 2a without compromising the sample structural integrity (see Figure S1d, Supporting Information). This was confirmed by the complete disappearance of the 905 cm^{-1} bands (epoxy) and the appearance of the amine-related bands in the region between 3600 and 2800 cm^{-1}. The degree of functionalization did not change significantly at shorter reaction times (see the curve to the right of Figure 2a). Hence, 30 s was established as the MW treatment time to functionalize PEGDA250/GMA samples with the PEI600 solution. Considering the molecular structure of the three amines used (DETA, PEI600 and PEI10k), one should forecast differences in reactivity due to the steric hindrance of the polymer backbone of these aliphatic amines, which limits the accessibility to the surface reactive groups for the primary and secondary amines in more hyperbranched molecules, as demonstrated elsewhere.[34] Hence, for the PEI10k solution, we expect longer MW irradiation times (>30 s) and shorter or similar irradiation times (≥30 s) using the DETA solution. Accordingly, the minimum MW treatment time using the PEI10k solution was found to be 15 min, see Figure 2b. Even if this time of irradiation is much higher than for PEI600-treated samples, it is considerably shorter than conventional methods using mechanical stirring (requiring more than 24 h of continuous stirring at ambient temperature to reach a similar degree of functionalization, see Figure S4, Supporting Information). After 15 min of MW irradiation time, the samples ended up with significant brittleness. Hence, for future experiments in which the functionalization with PEI10K is required, particular care is necessary for handling the treated samples. In the case of the highly reactive DETA, even though the plateau was reached after only 10 s of irradiation, the reaction time was set as 30 s, to minimize possible irregularities in MW power in such a short period (see Figure 2c).

The results for epoxy/acrylate conversion in all formulations are summarized in **Table 2**. Samples with higher epoxy content presented the greatest increase in the amine band; furthermore, higher intensity values for the amines with higher molecular weight (hyperbranched PEI600 and PEI10k). In general, the acrylate conversion from the 3D printed samples increased significantly (up to near 100%) after the MW treatments, depending on the sample's composition and the type of amines used (Table 2). At the same time, the ring-opening reaction took place, quantitatively, for all the samples. The slight differences in the epoxy conversion between the samples are related again to the molecular weight of the amines. The differences can be related to the

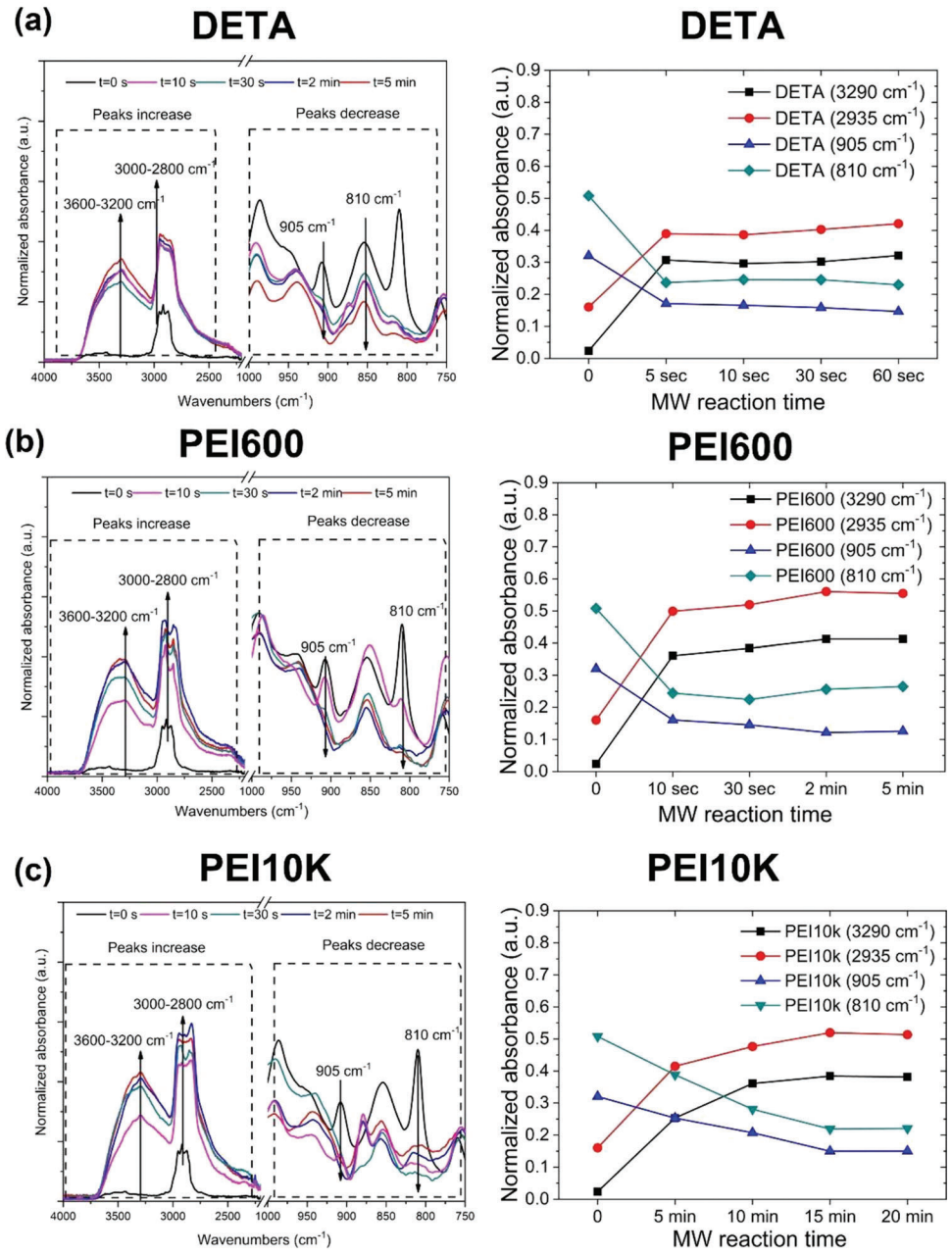

Figure 2. ATR-FTIR spectra and variation of intensity of the significant bands of the 3D printed 5:5 PEGDA250/GMA samples after the microwave-induced functionalization at different MW irradiation times: a) PEI600 solution, b) PEI10k solution, and c) DETA solution. Variation in acrylate bands has been corrected by subtraction of the thermal contribution of the MW radiation (see explanation in Figure S3, Supporting Information).

topological restriction of the aliphatic amines used, which hinders access to N–H bonds, and the different reactivity of primary and secondary amines, as demonstrated in literature.[30]

Figure 3a shows the evolution of the absorbance intensity obtained associated with N–H bonds (3600–3200 cm^{-1} region) and C–H bonds (3000–2800 cm^{-1} region) from treated PEGDA250/GMA samples. Some trends can be observed: 1) the formulation with higher glycidyl content reacts with more amine molecules, producing a considerable increase in the amine-related regions' absorbance intensity due to a higher amount of amine groups on the sample's surface. 2) The absorbance intensity of these regions is greater according to the type of amine used, reaching higher values for the highest molecular weight hyperbranched amines PEI600 and PEI10k (see also Figure S5, Supporting Information).

The change in surface polarity of the MW-treated samples was evaluated by contact angle measurements for all samples as the reaction proceeds, see Figure 3b (and Table S2, Supporting Information). All the tested samples showed an increase of hydrophobicity related to MW treatment, which can be related both to

Table 2. Acrylate double-bond and epoxy conversions of 3D printed PEGDA250/GMA and PEGDA250 samples before and after microwave-assisted functionalization with DETA solution (30 s of MW time), PEI600 solution (30 s of MW time), and PEI10k solution (15 min of MW time). Infrared spectra of the signals of interest for the different samples are shown in Figure 3.

Samples	As 3D printed	After microwave treatments					
	Acrylate conversion [%]	Acrylate conversion [%][a]			Epoxy conversion [%][b]		
		DETA	PEI600	PEI 10k	DETA	PEI 600	PEI10k
PEGDA250	82	85	83	87	-	-	-
9:1 PEGDA250/GMA	83	87	92	91	96	97	95
7:3 PEGDA250/GMA	85	96	96	97	98	98	98
5:5 PEGDA250/GMA	90	96	98	91	97	98	98

[a] The acrylate conversion was evaluated following the C=C signal at 810 cm^{-1} in comparison with the initial area of the same peak in the uncured formulation; [b] The epoxy conversion was evaluated following the glycidyl band at 905 cm^{-1} in comparison with the initial area of the same peak in the uncured formulation.

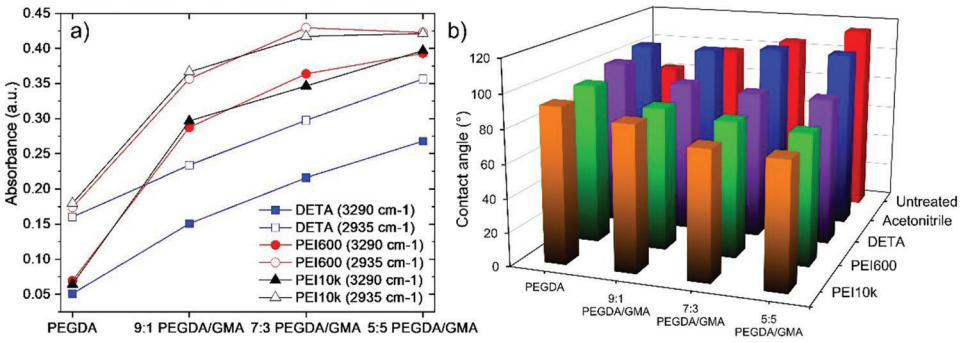

Figure 3. a) Normalized absorbance intensity as a function of the PEGDA250/GMA weight ratios after the different microwave treatments. Filled symbols refer to the 3600–3200 cm^{-1} region's absorbance, associated with amines' N–H bond stretching. Empty symbols refer to the 3000–2800 cm^{-1} region's absorbance associated with the C–H bond. b) Histogram showing the static contact angle of untreated and MW-treated samples as a function of the PEGDA250/GMA weight ratios and after the different MW-treatment treatments. The entry named "acetonitrile" indicates specimens that were subjected to MW treatment in the solvent without amines.

reaction of surface groups and to small surface modifications. When grafting amines, more hydrophilic surfaces were obtained and the contact angle decreases more when hyperbranched amines are used as modifiers (e.g., PEI10k and PEI600). Furthermore, the more the GMA in the formulation, the lower was the contact angle. These results are in good agreement with FTIR experiments. The lowest contact angle value is found for the 5:5 PEGDA250/GMA formulation, then confirming the highest surface modification due to both the higher content and reactivity of the glycidyl functional group. A more detailed discussion of these data is reported in the Supporting Information file.

2.3. Antibacterial Evaluation

The incorporation of amino functionalities over the 3D printed PEGDA250/GMA samples can introduce antibacterial features, given the known antimicrobial characteristics of amines.[35,36] Hence, the antimicrobial properties of the amine-treated 3D printed samples were tested against *S. aureus*. This bacteria model is known to be responsible for many infections-related diseases.[37,38] As previously discussed, the MW-treatment can introduce modification in the samples, which in some cases might lead to sample cracking and breaking (principally on 5:5 PEGDA250/GMA samples). This situation can adversely affect the antibacterial studies since such defects might be points where bacteria can host and grow; therefore, the antibacterial tests may not be reproducible. Based on this observation, the antibacterial evaluation was performed only on MW-treated 9:1, 7:3 PEGDA250/GMA and PEGDA250 samples.

The bacterial line was seeded on flat 3D printed samples and the bacterial growth was monitored by taking photographs at 24 and 48 h with an optical microscope using 20× magnification. *S. aureus* strain can be identified due to its characteristic round morphology. Photographs for PEGDA250 matrices treated with the different amine solutions are shown in **Figure 4**a (while the photographs for the other tested materials are shown in Figure S6, Supporting Information). After 24 h, bacteria colonization was evident in all tested samples despite their neither matrix composition nor type of amine functionalization, with no clear difference between treated and untreated samples. The colonization increased at 48 h due to colony proliferation along the surfaces, confirming the proposed seeding strategy.

When surfaces were analyzed with the Live/Dead assay, the results are rather different between control and amine-functionalized films. The effect of the different surface functionalizations on bacteria viability for PEGDA250 samples can be seen in Figure 4b,c (for the rest of the samples, see Figure

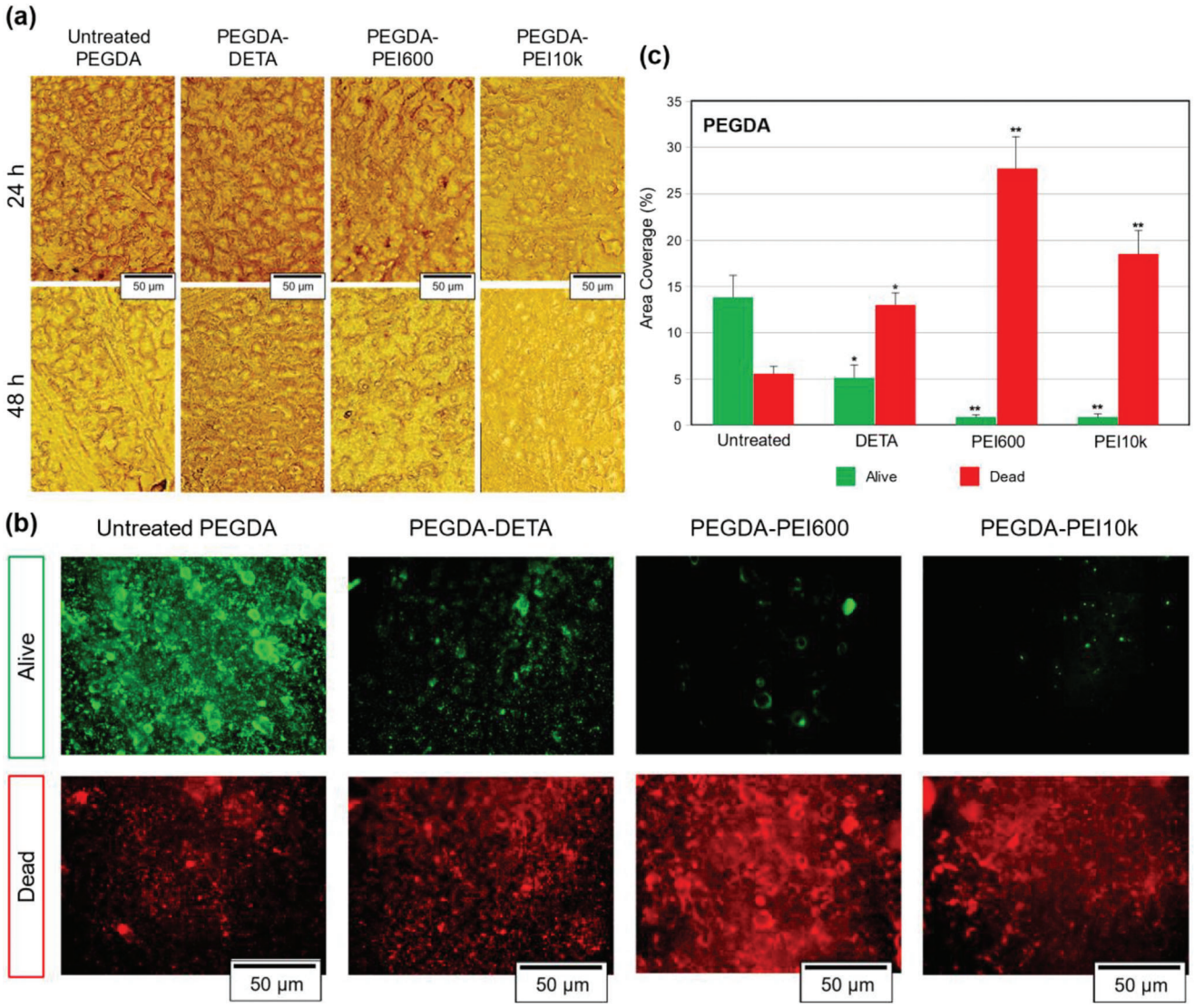

Figure 4. a) Photographs in bright field of bacterial growth and colonization on 3D printed PEGDA samples at 24 and 48 h for untreated and MW-treated samples with DETA, PEI600 and PEI10k solutions. b) Photograph of alive (green) and dead (red) bacteria over 3D printed PEGDA250 samples and c) the respective quantification of percentage (%) of the area covered by alive and dead bacteria over the samples' surface. Green bars represent % coverage of alive bacteria; red bars represent % coverage of dead bacteria. One asterisk (*) corresponds to p-value <0.05 and two asterisks (**) corresponds to p-value <0.005.

S7, Supporting Information), in which alive bacteria are stained green and dead bacteria in red. In general, the antibacterial activity was marked more by the type of amine used for the MW treatment rather than the PEGDA/GMA polymer composition. For the three typologies of samples, the trend for the effect of the different amines on the surface was the same: a higher number of dead bacteria were found for samples treated with hyperbranched amines (PEI600 and PEI10k), where practically no alive bacteria were being observed. To exclude the combined effects of the rest of the parameters of the MW treatment reaction (e.g., temperature, solvent, and microwave irradiation) on antibacterial activity of surfaces, control PEGDA250 samples were immersed in pure acetonitrile and MW irradiated in the absence of any amine. The results were compared with untreated PEGDA samples and with MW-treated ones with PEI600 solution. No significant bacterial death was obtained (see Figure S8a,b, Supporting Information).

As mentioned above, surface irregularities could be starting points to promote the accumulation and colonization of bacteria. Indeed, in Figure S8c, Supporting Information is appreciated the bacteria pattern in imperfections observed by optical microscopy, which confirms that bacteria prefer to grow and accumulate in the nooks of uneven surfaces rather than on flatter ones. With these observations and results obtained, the best antimicrobial activity was obtained using hyperbranched amine solutions (PEI600 or PEI10k) for the MW functionalization steps regardless of the starting matrix composition employed. However, since polymeric matrices with GMA content are quite susceptible to the MW-treatment (that might generate points for growth and

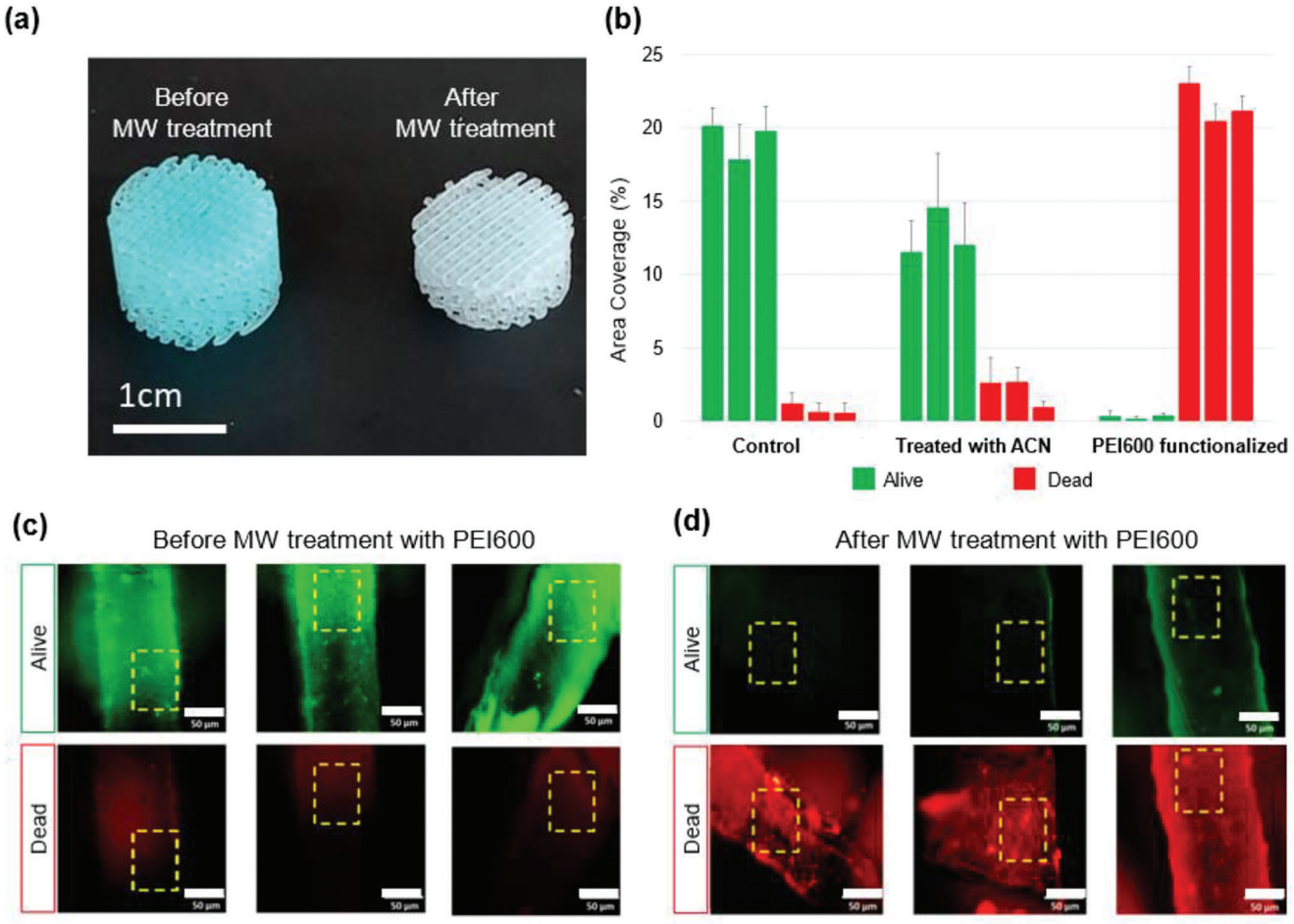

Figure 5. a) Optical images of two filter-type structures, as printed and after MW-assisted surface functionalization. b) Area percentage covered by dead (red) and alive (green) bacteria in three different slices for each sample composition: control (untreated), treated with only acetonitrile, and functionalized with PEI600. Photographs of dead (red) and alive (green) bacteria acquired from different slices of filter-type samples: c) control (scale bar equal to 50 µm.) and d) PEI600-functionalized (scale bar equal to 50 µm) samples.

colonization of bacteria), we selected the combination of PEGDA matrix and PEI600 functionalization for the following test. The surface of these samples was also analyzed by FESEM. Pristine 3D printed PEGDA clearly shows layering of 100 µm related to DLP process (Figure S9a, Supporting Information) and rather smooth surface, even if some wrinkling is present perpendicularly to the build direction, probably related to pixeling (Figure S9b, Supporting Information). Those are even more evident in the PEI600 sample (Figure S9c,d, Supporting Information), even if the surface does not seem greatly affected, but probably sufficiently to promote bacteria accumulation.

2.4. Filter-Type Functionalization and Biocidal Activity

Filter-type structures were designed (CAD file in Figure S10, Supporting Information) and fabricated with the geometry described in the experimental section to serve as an example of a complex-shaped 3D printed object, and to explore the viability of our strategy to modify intricate surfaces (width of the struts 100 µm). 3D printed PEGDA250 structures, were surface functionalized with PEI600 solution, following the same procedure as for flat samples (30 s of MW treatment in ACN), but adding two sonication steps: a first sonication step (8 min) with the reactive PEI600 solution before the MW treatment to assure the complete filling of the internal voids, and a second sonication step (10 min) in water, for the complete cleaning after MW reaction. Following that procedure, surface-anchoring of PEI600 was attempted. Two specimens (untreated and MW treated structures) are shown in **Figure 5**a; the slight color change was due to release of BG in water during MW treatment, while no evident damages are observed.

After the reaction, the samples were cut into five 1 mm slices, seeded with *S. aureus* and studied by Live/Dead assay. Images of the seeded slices samples (control and functionalized) are shown in Figure 5c,d. As observed, all MW-treated slices showed the same antibacterial activity, thus, successful functionalization of the surface along the *z*-axis of the structures was achieved. The photographs concerning the control slices (Figure 5c) showed the presence of almost exclusively alive bacteria, whereas on functionalized slices with PEI600 (Figure 5d) the surface is covered by only dead bacteria, and no living bacteria were observed. In addition, the PEI600 functionalization of the samples was found to

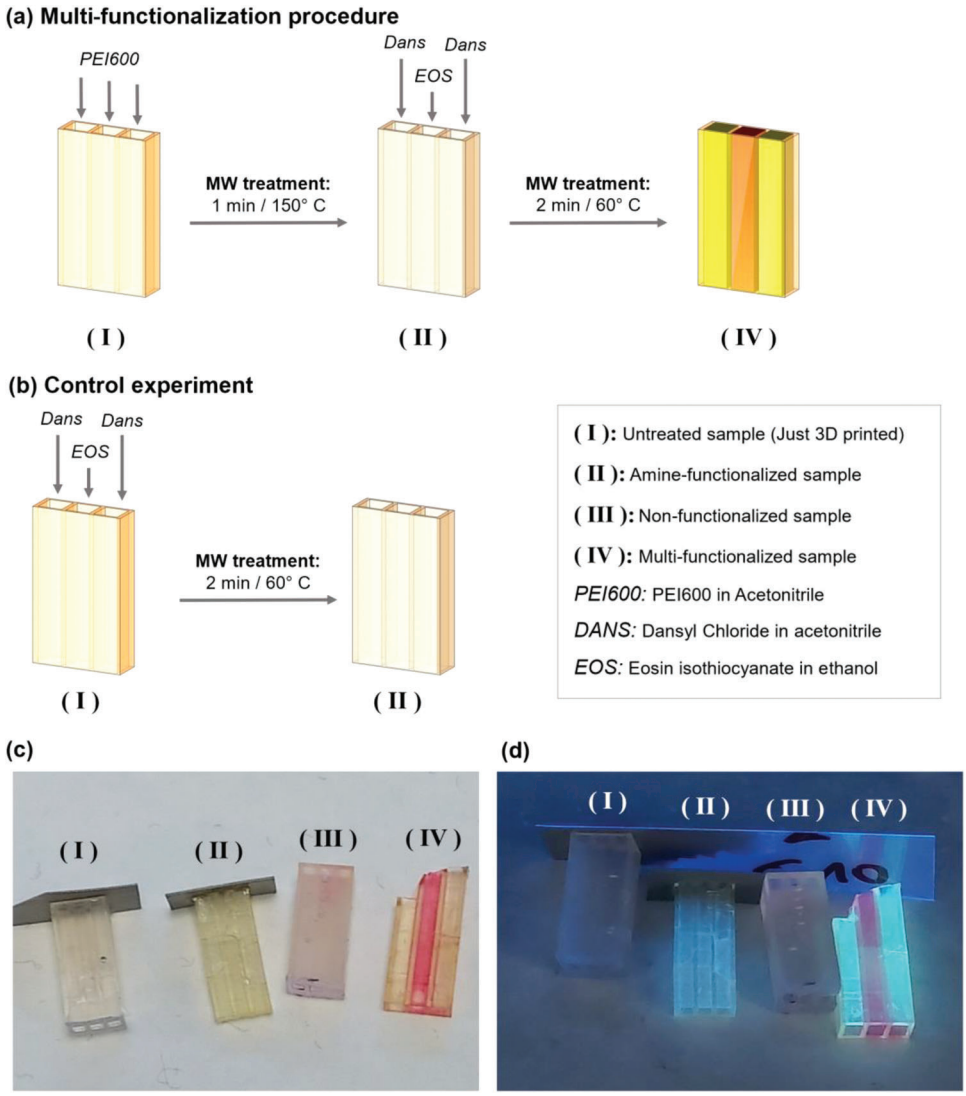

Figure 6. a) Scheme of the functionalization procedure with the PEI600 solution and Dansyl (Dans) and Eosin (EOS) dye solution. b) Sketch of the control experiment. Photographs of the different MW-treated samples, that is, (I), (II), (III), and (IV) under c) visible light and d) UV light. Notation of the samples is in (a).

be homogeneous along the *z*-axis, as the percentage of alive/dead bacteria is maintained constant (Figure 5b).

2.5. Simultaneous Multi-Functionalization of 3D Structures

At last, the versatility of the proposed MW-assisted functionalization strategy has been demonstrated by performing a multi-functionalization procedure on the same 3D printed component. The concept is to attach, simultaneously, different types of molecules in the same 3D printed specimen through a single MW reaction procedure. Therefore, as a proof of concept, 3D printed fluidic devices, made of PEGDA, were fabricated consisting of three parallel millimetric channels of 2.4 × 2.4 mm (see Figure S11, Supporting Information). For this experiment, no dye was used for the sample 3D printing fabrication, aiming to have good optical transparency after the MW functionalization.

The procedure is sketched in **Figure 6**a. As shown, the functionalization procedure consists of two MW-assisted reaction steps: the 3D printed specimen (**I**) was first subjected to a MW-treatment of functionalization with the PEI600 solution at 150 °C for 1 min. Then, the channels of this amine-treated sample (**II**) were filled with the dye solutions (dansyl chloride and eosin isothiocyanate solutions), and MW irradiated again, this time, at 60 °C for 2 min, obtaining a sample with multiple functionalities (**IV**). These dyes were chosen because they are reactive with amines and they show very intense fluorescence and visible color respectively, hence, the success of the reaction can be easily detected by the naked eye and UV–vis illumination. As a control experiment (see Figure 6b), a 3D printed PEGDA sample was directly filled with the dyes solution (non-previously treated with amine) and MW treated at 60 °C for 2 min (**III**).

The multiple and independent functionalization of the three channels of the sample (**IV**) is evident by the change in color

and the fluorescence emission, as shown in Figure 6c,d, respectively. Moreover, the sample treated with dyes but not previously surface-modified with PEI600 (sample **III**), does not show any evidence of reaction (it did not show any color or fluorescence emission). Noteworthy, the further MW treatment between steps **III** and **IV** do not affect the surface of 3D printed, as evidenced in field emission scanning electron microscopy (FESEM) measurements (Figure S12a,b, Supporting Information). Furthermore, EDX analyses confirm the proposed reaction scheme, evidencing an increase of nitrogen in the tested samples (Table S3, Supporting Information).

Finally, as the dyes bear different functional groups (acyl chloride and isothiocyanate) those reactions could be used as models for the covalent functionalization of a broad range of amine-reactive fluorescent probes to a surface. Moreover, the reactions with Dansyl and Eosin dyes were performed using different solvents (acetonitrile and ethanol, respectively), so the possibility of using the best solvent for each reaction in each channel opens the versatility of this strategy.

3. Conclusion

In conclusion, a series of photopolymers made from different concentrations of PEGDA250 and GMA monomers (5:5, 7:3, 9:1, and 10:0) were successfully used for fabricating simple and complex-shaped samples through light-based 3D printing methods. These 3D printed specimens presented unreacted epoxy and acrylate functional groups onto their surface that were exploited for surface modification of such polymeric structures in a suitable post-printing protocol. In particular, the specimens were functionalized under microwave (MW) irradiation and using liquid solutions containing aliphatic polyamines. This microwave-assisted chemical functionalization was achieved via the nucleophilic attack of the N atom's electron pair to epoxy and acrylate groups. The amines used were poly-ethyleneamine derivatives, (i.e., diethylenetriamine and two types of hyperbranched polyethyleneimines), differing in molecular weight, architecture, and reactivity. The MW-treated samples presented changes in their surface properties due to the grafting of amines, which was evaluated via the ATR-FTIR method and static contact angle analysis and further confirmed by FESEM and EDX analysis. The MW-assisted surface functionalization developed in this work has been used for proofing two different purposes: first, an easy, rapid, and complete functionalization of complex 3D architectures, by measuring the antimicrobial activity against *S. aureus* of different parts of the functionalized specimens; and second, to perform simultaneous and independent functionalization of single channels of such specimens.

With the microwave-assisted functionalization developed in this work, the surface features of 3D printed can be enhanced and customized according to the envisaged properties of the structures. The combination of material preparation versatility and freedom of design of light-based 3D printing with an easy MW-assisted functionalization strategy might widen the palette of possibilities of 3D printing for many scientific and technological fields. In particular, the findings here reported can be of great interest in biology and biotechnology fields, in which surface properties can be engineered to fabricate antibacterial objects (e.g., active air filters) or with preferential cellular adhesion. Another field of interest can be in sensors, and in particular in the use of luminescent sensors grafted in microfluidics. On the other hand, the strategy presented can be in general employed in all the applications where the surface characteristics of the printed parts are a key point for successful operations and evaluations.

4. Experimental Section

Materials: Poly(ethylene) glycol diacrylate (PEGDA250, M_n = 250 g mol^{-1}), glycidyl methacrylate (GMA, M_n = 142.15 g mol^{-1}), phenyl bis(2,4,6-trimethylbenzoyl)phosphine oxide (BAPO, 97%), disperse red one methacrylate (DR1-MA, 95%), brilliant green (BG, ≈90%), diethylenetriamine (DETA, M_w = 103.17 g mol^{-1}), two types of hyperbranched polyethyleneimine (PEI600, M_n ≈ 600 g mol^{-1}) and 10 kDa (PEI10k, M_n ≈ 10 000 g mol^{-1}), dansyl chloride (98%), eosin isothiocyanate (95%), ethanol (99.8%), and acetonitrile (≥99.8) were purchased from Merck Company (Darmstadt, Germany) and used as received. The ratio of primary/secondary/tertiary amine groups in DETA, PEI600, and PEI10k are 1:0.5:0, 1:0.82:0.53, and 1:1.2:0.76.[30,31]

Preparation of 3D Printable Formulations: Four photocurable formulations were prepared with different weight ratios between PEGDA250 and GMA monomers: 5:5, 7:3, 9:1, and 10:0, respectively. The molar ratio between PEGDA250 and GMA is reported in Table 1, the increasing amount of GMA was tested to check the effect of increasing the amount of epoxy groups in the functionalization step. Each formulation was prepared by mixing first the monomers and afterward adding 1 wt% of BAPO and 0.01 wt% of DR1-MA or BG dye (the selection of the dye was made for aesthetic reason for the images since both works well for 3D printing without interfere in the experiments).

The formulations were then mechanically stirred at room temperature until a complete homogeneous solution was obtained.

As 3D printing equipment, a Pico 2 HD DLP-3D printer (Asiga, Australia) provided with a LED light source (405 nm), nominal *XY* pixel resolution of 50 µm, and minimum *z*-axis control of 1 µm was used. The structures were produced by fixing a printing slicing of 50 µm and a light intensity of 20 mW cm^{-2}. The light exposure time was set according to the formulation used, as shown in Table 1. All CAD designs were produced with the FreeCAD program and exported in STL format. For the optimization of the MW-surface modification reactions, flat discs (150 µm thick and 9 mm in diameter) were 3D printed. For the simultaneous MW-assisted functionalization, samples were 3D printed (width 0.9 cm, thickness 0.3 cm, and height 1.5 cm) hosting three parallel channels (2.4 mm × 2.4 mm). The filter-type structures (diameter 0.9 mm and variable height) were also printed.

Microwave-Assisted Surface Functionalization Procedure: An Anton Paar Monowave Synthesis 300 microwave reactor provided with an infrared sensor (IR pyrometer) was used for the surface modifications. The reaction was performed under magnetic stirring inside a pressure-resistant 10 mL glass MW vial sealed with a silicon septum. For the MW-assisted modification reactions, five different amine-based solutions or reactive solutions were prepared:

1) *DETA solution*: Composed of diethylenetriamine in acetonitrile (33 mg mL^{-1}).
2) *PEI600 solution*: Composed of poly(ethylenimine) 600 Da in acetonitrile (33 mg mL^{-1}).
3) *PEI10k solution*: Composed of poly(ethyleneimine) 10 kDa in a 12:1 mixture of acetonitrile and ethanol (87 mg/6.5 mL). Such a proportion of ethanol was added to enhance the PEI10k miscibility.
4) *Dansyl solution*: Composed of dansyl chloride dye in acetonitrile (1.5 mg mL^{-1}).
5) *Eosin solution*: Composed of eosin isothiocyanate dye in ethanol (1.5 mg mL^{-1}).

The general procedure for MW-functionalization is as follows: the specimens were introduced in the pressure-resistant 10 mL glass vial, and 5 mL

of a specific reactive solution (DETA, PEI600, or PEI10k) were added. The vial was exposed to microwave irradiation at different times at 150 °C and then cooled down to 55 °C. Finally, the samples were exhaustively washed with ethanol and water, and dried under vacuum (−70 cmHg/45 °C) overnight. For the MW functionalization of filter-type samples, firstly, they were sonicated for 8 min until bubbles disappeared to assure that internal voids were filled with the PEI600 solution. After finishing the MW reaction, the samples were washed twice in distilled water under sonication for 10 min to remove unbounded reactive compounds and dried under vacuum (−70 cmHg/45 °C) overnight. Before antimicrobial evaluation, the functionalized and control filter-type samples were cut into slices of about ≈1 mm thickness to be analyzed individually and to check whether functionalization had occurred homogeneously along the monoliths' *z*-axis. Control samples were subjected to the same process but without PEI600 solution (i.e., immersion in pure ACN, sonication when needed, MW irradiation, washing, and drying). For the simultaneous MW functionalization experiments, the 3D printed fluidic devices were first surface-modified with PEI600 as described above. Afterward, they were glued onto an acetate film employing an epoxy adhesive, and the channels were filled with two different dye solutions: dansyl chloride in acetonitrile and eosin isothiocyanate in ethanol. Both compounds were selected because they are only reactive with amines, and not with acrylate or epoxy groups. The samples were then end-capped with the same bonding procedure explained above. Finally, the fluidic specimens (filled and closed) were introduced into the 10 mL glass vial (provided with a magnetic stirrer), containing 5 mL of distilled water and exposed to MW irradiation for 2 min at 60 °C. After this, end-capping was manually removed, and the specimens were exhaustively washed with ethanol and water and dried under vacuum at 45 °C overnight.

Characterization Methods: An FTIR spectrometer (Nicolet iS50, Thermo Scientific, Milano, IT) was used to calculate the conversion of epoxy and acrylate double-bonds on the samples at different experimental conditions. The spectra were collected on an attenuated total reflectance (ATR) system (Smart iTX). Epoxy conversions were calculated by analyzing the peak at 905 cm^{-1} related to the oxirane group's C–O deformation, while the acrylate double-bonds conversions were calculated by monitoring the peak at 810 cm^{-1}, which corresponds to the C=C bonds' twisting.[40] The spectra were collected with a resolution of 4 cm^{-1} averaging 32 scans for each spectrum in the wavenumber range of 650–4000 cm^{-1}. Furthermore, the surface properties of the microwave-treated samples were evaluated following the region associated with, O–H stretch (3600–3200 cm^{-1}), N–H bond stretching of primary (3600–3400 cm^{-1}) and secondary amines (3400–3200 cm^{-1}), and the region associated with C–H bonds (3000–2800 cm^{-1}). All IR spectra were normalized using the carbonyl peak at 1720 cm^{-1}.

Static contact angle measurements were performed on 3D printed flat samples after different microwave treatment conditions and untreated samples using a KSV instrument LTD with CAM 200 analyzer program (Helsinki, Finland) equipped with a Basler A602f-2 camera. The tests were performed at room temperature with the sessile drop technique. A 3 µL droplet of deionized water (72.1 mN m^{-1}) was placed onto the sample, and the static angle was measured immediately after drop deposition. The measurement was repeated five times for each sample.

The distribution of nitrogen onto the surface was evaluated by scanning electron microscopy (SEM) with energy dispersive X-ray analysis (EDX). A Bruker Nano equipment with XFlash Detector 5030 was used to investigate the relative concentration of nitrogen retained on the untreated and functionalized surfaces after reactions. A probe current of 2.0×10^{-9} A and an accelerating voltage of 15 kV were used. The spot size irradiated was ≈0.5 mm^2 for all specimens. To determine the relative nitrogen concentration on the specimen surface, X-ray net counts were obtained at three random locations for each specimen with a collection time of 30 s. Three specimens were used for each condition. Samples were metalized with Cr prior to be analyzed. From all samples, an X-ray map was obtained.

Bacterial Seeding: Before bacterial seeding, the samples were sterilized, by washing twice with distilled water for 10 min and irradiating with UV light (λ_{irr} = 365 nm) for 20 min for each side. Then the materials were washed twice with distilled water for 10 min and finally submerged in clean distilled water.

S. aureus (*subsp. aureus* ATCC 25923) were cultured in Nutrient Broth No. 3 media (Sigma-Aldrich) at 37 °C overnight and under constant shaking at 125 rpm. The solution's optical density (O.D) was measured with a spectrophotometer at λ = 600 nm (Specord 205, Analytic Jenna) and used as a parameter to fix the bacteria concentration of the inoculum to a value of OD = 1.0 before seeding on the surfaces to ensure the reproducibility of the results. The bacteria were seeded on top of the flat surfaces and filter-type sample slices by adding 1 mL of *S. aureus* inoculum at OD = 1.0 to each sample, then incubated for 1 h at 37 °C. Afterward, the seeded surfaces were washed with distilled water to remove planktonic bacteria, and then the samples were incubated in distilled water to allow bacterial growth for 48 h.

Bacterial growth was monitored in the flat samples at 24 and 48 h with an inverted fluorescence microscope (Olympus I×51). Images were acquired under visible light using the bright field filter and 20× magnification. The control images were not performed on the filter-type slices due to their complex geometry, making it difficult to acquire pictures. Bacteria viability was measured at 48 h using the commercial L7007 LIVE/DEAD BacLight Bacterial Viability Kit (Molecular Probes). A 1:1 mixture of both dyes was prepared and diluted to 3 µL mL^{-1} in distilled water. Then 1 mL of the solution was added to each sample, followed by incubation in the dark at 37 °C for 15 min. Representative images were taken for each sample by triplicate using a fluorescence microscope with 20× magnification. Pictures of live and dead bacteria were acquired with FITC ($\lambda_{ex}/\lambda_{em}$ = 490/525 nm) and TRICT ($\lambda_{ex}/\lambda_{em}$ = 550/600 nm) filters, respectively. It is worth mentioning that each pair of pictures obtained for each sample corresponds to the same area. Bacteria quantification was done by analyzing % area coverage after a manual threshold had been set using the ImageJ software. The pictures obtained from the flat samples were divided into four quadrants over which the % area coverage was evaluated, whereas, for the filter-type specimens, only the best-focused image was used due to the inexistence of a flat plane.

Statistical Analysis: For bacteria coverage analysis, an unpaired Student's *t*-test between each sample and untreated control was performed. Statistical analyses were calculated using GraphPad Prism 4 software. One asterisk (*) corresponds to *p*-value <0.05 and two asterisks (**) corresponds to *p*-value <0.005.

Supporting Information

Supporting Information is available from the Wiley Online Library or from the author.

Conflict of Interest

The authors declare no conflict of interest.

Data Availability Statement

The data that support the findings of this study are available in theSupporting Information of this article.

Keywords

3D printing, antimicrobial materials, microwave-assisted reactions, simultaneous functionalization, surface functionalization

Received: March 30, 2023
Revised: May 30, 2023
Published online:

[1] *Green Technologies and Environmental Sustainability* (Eds: R. Singh, S. Kumar), Springer, Berlin **2017**. https://doi.org/10.1007/978-3-319-50654-8.

[2] S. C. Joshi, A. A. Sheikh, *Virtual Model. Rapid Manuf.: Adv. Res. Virtual Rapid Prototyping, Proc. Int. Conf. Adv. Res. Rapid Prototyping, 2nd* **2015**, *10*, 175.
[3] J. Sun, W. Zhou, D. Huang, J. Y. H. Fuh, G. S. Hong, *Food Bioprocess Technol.* **2015**, *8*, 1605.
[4] C.-K. Su, *Anal. Chim. Acta* **2021**, *1158*, 338348.
[5] C. W. Weyhrich, T. E. Long, *Polym. Int.* **2022**, *71*, 532.
[6] S. Park, W. Shou, L. Makatura, W. Matusik, K. (K.) Fu, *Matter* **2022**, *5*, 43.
[7] S. C. Ligon, R. Liska, J. Stampfl, M. Gurr, R. Mülhaupt, *Chem. Rev.* **2017**, *117*, 10212.
[8] F. Li, N. P. Macdonald, R. M. Guijt, M. C. Breadmore, *Lab Chip* **2019**, *19*, 35.
[9] G. Gonzalez, I. Roppolo, C. F. Pirri, A. Chiappone, *Addit. Manuf.* **2022**, *55*, 102867.
[10] M. Gastaldi, F. Cardano, M. Zanetti, G. Viscardi, C. Barolo, S. Bordiga, S. Magdassi, A. Fin, I. Roppolo, *ACS Mater. Lett.* **2021**, *3*, 1.
[11] J. S. Manzano, Z. B. Weinstein, A. D. Sadow, I. I. Slowing, *ACS Catal.* **2017**, *7*, 7567.
[12] M. A. Catterton, A. N. Montalbine, R. R. Pompano, *Langmuir* **2021**, *37*, 7341.
[13] P. Jiang, Z. Ji, X. Wang, F. Zhou, *J. Mater. Chem. C* **2020**, *8*, 12380.
[14] Y. I. Zhang, *Int. J. Bioprint.* **2017**, *3*, 001.
[15] M. J. Lerman, B. T. Smith, A. G. Gerald, M. Santoro, J. A. Fookes, A. G. Mikos, J. P. Fisher, *Tissue Eng., Part C* **2020**, *26*, 118.
[16] C. Cheng, M. Gupta, *Beilstein J. Nanotechnol.* **2017**, *8*, 1629.
[17] G. Gonzalez, A. Chiappone, K. Dietliker, C. F. Pirri, I. Roppolo, *Adv. Mater. Technol.* **2020**, *5*, 2000374.
[18] S. M. Mirabedini, H. Rahimi, S. H. Hamedifar, S. Mohsen Mohseni, *Int. J. Adhes. Adhes.* **2004**, *24*, 163.
[19] H. Mohandas, G. Sivakumar, P. Kasi, S. K. Jaganathan, E. Supriyanto, *Biomed Res. Int.* **2013**, *2013*, 253473 .
[20] S. Das, A. K. Mukhopadhyay, S. Datta, D. Basu, *Bull. Mater. Sci.* **2009**, *31*, 943.
[21] K. Malekshahinezhad, A. Ahmadi-Khaneghah, H. Behniafar, *Macromol. Res.* **2020**, *28*, 567.
[22] S. Mallakpour, A. Zadehnazari, *Prog. Org. Coat.* **2014**, *77*, 679.
[23] H. Gong, M. Beauchamp, S. Perry, A. T. Woolley, G. P. Nordin, *RSC Adv.* **2015**, *5*, 106621.
[24] M. Männel, C. Fischer, J. Thiele, *Micromachines (Basel)* **2020**, *11*, 246.
[25] S. Lantean, I. Roppolo, M. Sangermano, C. Pirri, A. Chiappone, *Inventions* **2018**, *3*, 29.
[26] C. Mukherjee, A. K. Misra, *Lett. Org. Chem.* **2007**, *4*, 54.
[27] G. Bosica, J. Spiteri, C. Borg, *Tetrahedron* **2014**, *70*, 2449.
[28] P. Kalita, C. D. Pegu, P. Dutta, P. K. Baruah, *J. Mol. Catal. A: Chem.* **2014**, *394*, 145.
[29] K. Johnston, S. K. Pavuluri, M. T. Leonard, M. P. Y. Desmulliez, V. Arrighi, *Thermochim. Acta* **2015**, *616*, 100.
[30] G. González, X. Fernández-Francos, À. Serra, M. Sangermano, X. Ramis, *Polym. Chem.* **2015**, *6*, 6987.
[31] E. M. Muzammil, A. Khan, M. C. Stuparu, *RSC Adv.* **2017**, *7*, 55874.
[32] A. Ozkomur, C. B. B. Fortes, *J. Appl. Biomater. Funct. Mater.* **2016**, *14*, e302.
[33] J. Karawatthanaworrakul, J. Aksornmuang, *J. Int. Dent. Med. Res.* **2020**, *13*, 29.
[34] B. D. Mather, K. Viswanathan, K. M. Miller, T. E. Long, *Prog. Polym. Sci.* **2006**, *31*, 487 .
[35] K. A. Gibney, I. Sovadinova, A. I. Lopez, M. Urban, Z. Ridgway, G. A. Caputo, K. Kuroda, *Macromol. Biosci.* **2012**, *12*, 1279.
[36] X. Meng, R. Xing, S. Liu, H. Yu, K. Li, Y. Qin, P. Li, *Int. J. Biol. Macromol.* **2012**, *50*, 918.
[37] J. Wang, J. Li, G. Guo, Q. Wang, J. Tang, Y. Zhao, H. Qin, T. Wahafu, H. Shen, X. Liu, X. Zhang, *Sci. Rep.* **2016**, *6*, 32699.
[38] D. S. Ondusko, D. Nolt, *Pediatr. Rev.* **2018**, *39*, 287.
[39] F. Román, P. Colomer, Y. Calventus, J. Hutchinson, *Materials* **2018**, *11*, 410.
[40] B. De Ruiter, A. El-Ghayoury, H. Hofmeier, U. S. Schubert, M. Manea, *Prog. Org. Coat.* **2006**, *55*, 154.

